HHS Public Access

Author manuscript

Connect Tissue Res. Author manuscript; available in PMC 2017 November 01.

Published in final edited form as:

Connect Tissue Res. 2016 November ; 57(6): 516–525. doi:10.3109/03008207.2015.1072519.

Synergistic enhancement of ectopic bone formation by supplementation of freshly isolated marrow cells with purified MSC in collagen–chitosan hydrogel microbeads

Joel K. Wise[1], **Andrea I. Alford**[2], **Steven A. Goldstein**[1,2], and **Jan P. Stegemann**[1]

[1]Department of Biomedical Engineering, University of Michigan, Ann Arbor, MI, USA

[2]Department of Orthopaedic Surgery, University of Michigan, Ann Arbor, MI, USA

Abstract

Purpose—Bone marrow-derived mesenchymal stem cells (MSC) can differentiate osteogenic lineages, but their tissue regeneration ability is inconsistent. The bone marrow mononuclear cell (BMMC) fraction of adult bone marrow contains a variety of progenitor cells that may potentiate tissue regeneration. This study examined the utility of BMMC, both alone and in combination with purified MSC, as a cell source for bone regeneration.

Methods—Fresh BMMC, culture-expanded MSC, and a combination of BMMC and MSC were encapsulated in collagen–chitosan hydrogel microbeads for pre-culture and minimally invasive delivery. Microbeads were cultured in growth medium for 3 days, and then in either growth or osteogenic medium for 17 days prior to subcutaneous injection in the rat dorsum.

Results—MSC remained viable in microbeads over 17 days in pre-culture, while some of the BMMC fraction were nonviable. After 5 weeks of implantation, microCT and histology showed that supplementation of BMMC with MSC produced a strong synergistic effect on the volume of ectopic bone formation, compared to either cell source alone. Microbeads containing only fresh BMMC or only cultured MSC maintained in osteogenic medium resulted in more bone formation than their counterparts cultured in growth medium. Histological staining showed evidence of residual microbead matrix in undifferentiated samples and indications of more advanced tissue remodeling in differentiated samples.

Conclusions—These data suggest that components of the BMMC fraction can act synergistically with predifferentiated MSC to potentiate ectopic bone formation. The microbead system may have utility in delivering desired cell populations in bone regeneration applications.

Keywords

Bone formation; bone marrow mononuclear cells (BMMC); chitosan; collagen; ectopic; hydrogel; mesenchymal stem cells

Correspondence: Jan P. Stegemann, Ph.D. Department of Biomedical Engineering, University of Michigan, 1101 Beal Ave., Ann Arbor, MI 48109, USA. Tel: +(734) 764-8313. Fax: +(734) 764-8313. jpsteg@umich.edu.

Declaration of interest: The authors report no conflicts of interest. The authors alone are responsible for the content and writing of the paper.

Introduction

Enhancement and acceleration of *in vivo* bone regeneration is often required to repair large bone defects resulting from trauma, disease, or tumor resection. The current clinical standard in these cases is autologous bone grafting, however there is a need for improved solutions. Stem cell-based therapies have shown promise in enhancing bone regeneration, often in combination with biomaterial carriers. Marrow-derived multipotent mesenchymal stem cells (MSC) are commonly investigated in the context of bone regeneration (1–3), due to their well-established self-renewal and osteoblastic differentiation potential. In addition, these cells exhibit important trophic and immunosuppressive activities that enhance the regenerative microenvironment (4). For bone regeneration applications, MSC are typically expanded *in vitro* to obtain large numbers of cells, but this process is time-consuming and is predicted to have high labor demand and facility costs for clinical-scale manufacturing (5). Additionally, it has been reported that culture expansion of MSC can diminish proliferation rate, multi-lineage differentiation potential, and bone-forming efficiency *in vivo*, compared to fresh bone marrow-derived MSC (6).

An alternative to using purified and cultured MSC is to deliver either whole or partially fractionated bone marrow to harness the reparative capacity of both the resident progenitor and support cells. The bone marrow mononuclear cell (BMMC) fraction consists of a heterogeneous population of cells, including MSC, hematopoietic stem/progenitor cells, endothelial progenitor cells, pericytes, adipocytes, macro-phages, monocytes, neutrophils, and platelets. Using fresh BMMC for bone tissue engineering has the potential advantage of leveraging the positive effects of paracrine signals and bioactive factors provided by the heterotypic marrow-derived cells to promote osteoinduction of marrow-derived MSC (7–11). It has been demonstrated that the combination of BMMC with biomaterials can lead to bone formation in a subcutaneous ectopic site (6,12–17). In contrast, other studies have suggested that ectopic bone formation *in vivo* is best potentiated using pre-cultured and pre-differentiated MSC, and that fresh marrow and BMMC are less effective in this regard (18,19). In our own work, we have demonstrated previously that BMMC show a similar degree of osteogenesis as culture-expanded MSC when encapsulated within 3D collagen-chitosan microenvironments, even though the fresh BMMC preparations initially contain an order of magnitude fewer MSC (20).

In the present study, we tested and compared the *in vivo* bone formation capacity of freshly isolated BMMC, culture-expanded MSC, as well as a combination of BMMC supplemented with MSC. Cells were delivered in modular 3D collagen-chitosan hydrogel microbeads, which we have shown previously to serve as osteoconductive microenvironments, (20,21-23) and which can be delivered minimally invasively via injection (22). A well-established ectopic subcutaneous implantation model (24) was chosen to evaluate the capacity of pure and mixed cell populations to generate mineralized tissue. The primary endpoint was bone formation volume and quality at the ectopic implant site at 5 weeks, as assessed by microcomputed tomography (microCT) and histology.

Materials and methods

Isolation of rat bone marrow-derived MSC

Six Fischer rats (3–6 weeks old) were euthanized using carbon dioxide inhalation prior to harvesting both femur and tibia. The distal and proximal ends of each femur and tibia were removed and the marrow was flushed out with sterile culture media. A single cell suspension was prepared by mechanical disruption and filtered using a 70 μm cell strainer (25). BMMC were plated at 5×10^5 cells/cm^2 and cultured in MSC growth media consisting of α-MEM (Gibco, Grand Island, NY), 10% fetal bovine serum (FBS; HyClone MSC screened), and penicillin (5000 units/100 ml)/streptomycin sulphate (5mg/100ml) (P/S, Gibco, Grand Island, NY). Cultures were maintained in a standard cell culture incubator at 37 °C with 5% CO_2. Culture medium was changed every 3–4 days and adherent rat marrow-derived MSC were culture expanded until passage 4, at which point the cells were used for hydrogel microbead experiments. Prior to encapsulation, cell numbers were determined using an automated cell counter (Beckman Coulter, Pasadena, CA).

Harvest of freshly isolated rat BMMC

A single cell suspension was obtained from an additional six Fischer rats as outlined above. Red blood cells (RBC) were lysed using an ammonium chloride-based lysis buffer (26–28) containing 150 mM NH_4Cl, 10 mM $KHCO_3$, and 0.1 mM EDTA (all from Sigma-Aldrich, St. Louis, MO). A fresh rat bone marrow cell suspension in 30 ml of MSC growth media was mixed with 60 ml of RBC lysis buffer (1:3 dilution) for 7 min at room temperature. Cells were centrifuged at 3500rpm for 2min, washed with sterile PBS, and the collected BMMC were resuspended in 20 ml of MSC growth media. Prior to directly seeding fresh uncultured BMMC into hydrogel microbeads, BMMC numbers were determined using an automated cell counter (Beckman Coulter, Pasadena, CA). Cells were centrifuged at 200 *g* for 5 min, and then resuspended in MSC growth media.

Fabrication of collagen–chitosan hydrogel microbeads

Collagen–chitosan hydrogel materials were prepared at a mass ratio of 65–35 wt% as described previously (20,23). Briefly, each 12 ml collagen–chitosan hydrogel preparation consisted of: 6000 μL collagen type 1 (4.0mg/ml in 0.02 N acetic acid, MP Biomedicals Inc., Santa Ana, CA), 660 μL chitosan (2%wt/vol in 0.1N acetic acid, Novamatrix Inc., Philadelphia, PA), 1460 μL β-glycerophosphate (580mg/ml in water, Sigma-Aldrich, St. Louis, MO), 140 μL glyoxal (87.5 mM in water, Sigma-Aldrich, St. Louis, MO), and 3740μL of cell suspension in MSC growth media. All components were kept on ice before being mixed to create a liquid matrix formulation containing suspended cells. Three types of cell–hydrogel mixtures were used in this study: “F” preparations containing freshly isolated BMMC (passage 0) at a concentration of 25×10^6 cells/ml, “C” preparations containing culture-expanded rat marrow-derived MSC (passage 4) at a concentration of 5×10^5 cells/ml, and “F + C” preparations containing a combination of both freshly isolated BMMC at a concentration of 3×10^6 cells/ml and culture-expanded MSC at a concentration of 5×10^5 cells/ml. A fourth hydrogel mixture containing no cells was prepared to serve as an acellular control, and is designated the “A” preparation. Hydrogel microbeads were fabricated using a water-in-oil emulsion method described previously (20,23). Briefly, the

liquid cell–hydrogel mixture was injected into a 100 cS polydimethylsiloxane bath (PDMS, Xiameter Inc., Dow Corning, Midland, MI) under constant stirring using a mixing apparatus (Barnant Co., Vernon Hills, IL) with a custom impeller. Emulsification was carried out by mixing at 800 rpm while the PDMS was maintained cold in a crushed ice bath for 5 min. Once the liquid matrix droplets were fully emulsified and homogenously mixed, the PDMS bath was transferred to a water bath at 37 °C for 25 min with constant stirring to initiate thermal gelation and to achieve co-polymerization of collagen–chitosan microbeads. The resulting cell-encapsulating microbeads were collected from the PDMS phase by centrifugation at 200 *g* for 5 min and washed three times with MSC growth media and centrifugation.

In vitro culture of collagen–chitosan hydrogel microbeads

All microbead preparations were cultured *in vitro* in MSC growth medium for an initial 3 days at 37 °C and 5% CO_2. Subsequently, culture media was changed by centrifuging at 200 *g* for 5 min, aspirating media from collected microbeads, and adding either MSC growth media (referred to as media type "G") or osteogenic differentiation media (referred to as media type "O") to the appropriate samples. The time point of this initial medium change is designated as day 0. Osteogenic differentiation medium consisted of control medium (α-MEM, 10% FBS, 1% P/S) supplemented with 0.2 mM L-ascorbic acid 2-phosphate, 10 mM β-glycerophosphate, and 100 nM dexamethasone (all from Sigma-Aldrich, St. Louis, MO). The resulting types of microbead samples were designated by their cell content and medium type used: "A_G", "F_G", "F_O", "C_G", "C_O", "F + C_O" (see Figure 1 for key). All culture media were changed every 3 days by centrifugation of microbeads at 200 *g* for 5 min, aspiration of used medium, and replenishment with fresh medium. Microbead samples were cultured *in vitro* in either growth or osteogenic media for 17 days.

Imaging and characterization of cells and microbeads

At day 14, cell viability within microbeads was assessed using a commercially available vital staining kit (Molecular Probes, Eugene, OR). A small portion of microbeads was obtained from each sample type and washed twice in sterile PBS for 10 min, then incubated at 37 °C for 45 min in a solution containing 4.0 μm calcein-AM and 4.0 μm ethidium homodimer-1 in PBS. Calcein-AM diffuses across the membrane of live cells and reacts with intracellular esterases to emit bright green fluorescence, while ethidium homodimer-1 can enter only dead cells with damaged cell membranes and emits bright red fluorescence upon binding to nucleic acids. After resuspension in PBS, microbeads were imaged using laser scanning confocal microscope (Olympus America Inc., Center Valley, PA). At least three different and random views of dispersed microbeads were imaged at z-resolution of 6 μm, using FITC (ex = 494, em = 517nm) and PI (528/617 nm) filters. Transmitted light imaging captured the matching view of the microbeads which encapsulated the imaged live/dead fluorescent cells, in order to show morphology, size, and opacity of microbeads.

Delivery of 3D collagen–chitosan hydrogel microbeads to subcutaneous site

All implants were performed under a University of Michigan Animal Care and Use Committee approved protocol. Each of the six adult male Fischer rats received the same procedure of dorsal subcutaneous injectable implants of six microbead/fibrin gels using

aseptic technique. Figure 1 shows a schematic of the six types of microbead implants, where A = acellular, F = freshly isolated BMMC, C = culture-expanded MSC, G = growth medium, and O = osteogenic medium. Implantation was performed under inhalation anesthesia using isoflurane. The animals were placed in a prone position, and the dorsal surface was shaved and scrubbed with Chlorhexadine and saline using standard aseptic technique. Microbead samples (shown in inset images in Figure 1) were centrifuged at 200*g* for 5 min, resuspended in 177.5 μl of serum-free α-MEM, and then mixed with 312.5 μl of 4.0 mg/ml fibrinogen solution in serum-free α-MEM (Sigma-Aldrich, St. Louis, MO) and 10 μl of 50U/ml thrombin (Sigma-Aldrich, St. Louis, MO). After 15 s, the injectable implant mixture was drawn into a 1 ml syringe fitted with a 21 G needle. After 1 min, the contents of the syringe were injected subcutaneously into the appropriate site on the rat dorsum. The placements of implants were rotated for each rat, to account for any anatomical variability.

Harvest of microbead implants from subcutaneous site

At the 5-week time point, each microbead implant was harvested from its *in vivo* site. Rats were euthanized using carbon dioxide (CO_2) inhalation. A large incision was made along the spine and dorsal subcutaneous skin flaps were made to allow for visualization and harvesting of the implant. Microbead implants were carefully trimmed from the surrounding soft tissue, fixed in 10% buffered zinc formalin solution (Anatech Ltd., Battle Creek, MI) for 2 days at 4 °C, and stored in 70% ethanol.

Microcomputed tomography (microCT) imaging and analysis

To calculate the total bone/mineralized tissue volume (BV) and tissue mineral density (TMD) in each microbead implant specimen, microCT scanning and image analysis were used. The fixed specimens were securely held in a specimen holder while immersed in 70% ethanol. All samples were scanned via an *ex vivo* microCT specimen scanner (GE Healthcare Pre-Clinical Imaging, Milwaukee, WI) using 80 kV energy (X-ray voltage) and reconstructed on 18 -μm isotropic voxels with 18-μm thick slices. A calibration standard was used to calibrate the densitometric quantification of all images, and the grayscale values were converted to Hounsfield Units using water, air, and an HA phantom. The dense material within the microbead implant specimens was identified as new ectopic bone formation since its density was within the density spectrum of bone. Analysis was performed using GE MicroView on 3D regions of interest interpolated from stacked 2D splines, which were defined by contrast of implant and new bone formation compared to the surrounding soft tissue. The Bone Analysis feature of the software was used and a threshold of 1200 was chosen for the gray scale value to define bone voxels for all specimens. BV and TMD were recorded for each microbead implant specimen.

Histology

Microbead implant specimens were decalcified in 0.5 M EDTA (pH 7.4) for 4 days at 4 °C, histologically processed and embedded in paraffin, and sectioned at 7 μm. Serial sections were stained with Hematoxylin and Eosin (H&E), Toluidine Blue O (Tol. Blue O), and for tartrate-resistant acid phosphatase positive cells (TRAP+). Low magnification images of all histological staining were selected to maximize the surface area and total number of microbeads shown in the sections for each implant type.

Statistical analyses

Data are reported mean ± standard error of the mean (SEM). Data were analyzed by one-way ANOVA and statistical significance was defined at a level of $\alpha \leq 0.05$.

Results

Morphology and size of 3D collagen–chitosan microbeads

Collagen–chitosan microbeads of each of the types examined in this study are shown in Figure 2. The top panels (Figures 2A–F) show microbeads that had been cultured for 17 days (after the initial 3 days in growth medium) and then imaged by transmitted light microscopy. Microbeads had a generally spheroidal shape with diameters in the range of approximately 100–200 μm. At day 17, microbeads containing pure MSC (C_G and C_O, shown in Figure 2D and E) tended to cluster together to form larger aggregates due to cell–matrix and cell–cell adhesion as MSC proliferated on the outside of the microbeads (see Figure 2J and K). Microbeads cultured in osteogenic medium (F_O, C_O, and F+C_O, shown in Figure 2C, E, and F) exhibited a darker and more opaque appearance than those cultured in growth medium, suggesting that the matrix had started to mineralize during *in vitro* culture.

Viability of cells encapsulated in 3D collagen–chitosan microbeads

Vital staining of MSC encapsulated for 17 days in microbeads is shown in the lower panels of Figure 2. Green staining indicates the cytoplasm of viable cells, while red staining shows the nucleus of dead cells. Acellular microbeads (A_G, Figure 2G) served as negative controls. Microbeads containing only fresh BMMC (F_G and F_O, Figure 2H and I) contained a mixture of live and dead cells, as was evident and described previously (20). The lower viability of BMMC in the microbeads is likely caused by the culture medium used for microbead culture, which was optimized for MSC culture rather than BMMC maintenance. Live cells cultured in growth media within F_G microbeads had a smaller and more rounded morphology, compared to the noticeably larger and spread live cells cultured in osteogenic media within F_O microbeads. Microbeads containing only cultured MSC (C_G and C_O, Figure 2J and K) contained predominantly live cells exhibiting spread morphologies, with markedly fewer dead cells. The F + C_O microbeads (Figure 2L) contained a combination of fresh BMMC and culture-expanded MSC cultured in osteogenic medium. These samples also contained a mixture of live and dead cells however the proportion of live cells was much higher than in the F_O microbeads, which did not contain cultured MSC. The live spread cells within F_O and F+ C_O microbeads exhibited a similar size and morphology to the culture-expanded MSC within C_G and C_O microbeads, suggesting that these cells are MSC derived either from the fresh marrow cell preparation or the cultured MSC component.

Bone volume and TMD of 5-week microbead implants

Samples were analyzed using microCT imaging at 5 weeks after implantation. MicroCT scans from all samples were analyzed quantitatively to determine bone (BV) and TMD, and aggregate data are shown in Figure 3. Microbeads containing a combination of fresh BMMC and cultured MSC (F + C_O) resulted in a marked and statistically significant stimulatory

effect on bone volume, compared to acellular microbeads (A_G) and those containing only fresh BMMC (F_G and F_O). Microbeads containing cultured MSC and maintained in osteogenic medium (C_O) showed a trend towards more bone formation than their counterparts cultured in growth medium (C_G), but were not statistically significantly different from these treatments (Figure 3A). TMD values were similar for all microbead implants (Figure 3B), revealing that the average density of mature mineral in voxels identified as bone was consistent within these types of microbead implants. Representative reconstructed scans are shown in Figure 4. All samples resulted in some degree of ectopic bone formation, except the microbeads containing cultured MSC maintained in growth medium (C_G, Figure 4D).

Histology

Histological examination of implants was performed at 5 weeks, and representative stained samples are shown in Figure 5. Hematoxylin and eosin (H + E) treatment resulted in pink staining of the collagen-based microbeads in all implant types, and dark blue staining of all cell nuclei, as well as calcium deposits in some microbead implants (top panels, Figure 5A–F). All implants contained noticeable populations of small inflammatory-like cells outside and between microbeads. The role of these cells is not clear from this analysis, but their presence was not correlated with ectopic bone formation. Microbead implants containing cells and cultured in osteogenic medium (F_O, C_O, and F+C_O) exhibited prominent dark blue staining of cell nuclei and bone-related matrix around the microbead populations. In contrast, acellular microbeads (A_G) and those containing either fresh BMMC or cultured MSC and maintained in growth medium (F_G and C_G) displayed abundant pink staining of collagen-based microbeads, with low to moderate staining of cellular material. Staining of sections with Toluidine Blue O (middle panels, Figure 5H–L) revealed cells and native matrix through dark blue staining, but stained the lab-fabricated collagen-based microbeads a light blue color. The most abundant dark blue staining was observed in the microbeads containing a combination of fresh BMMC and cultured MSC (F + C_O), presumably due to staining of osteoblastic cells and new bone matrix in and around the microbead implant. Microbeads containing fresh BMMC or cultured MSC and maintained in osteogenic medium (F_O and C_O) also exhibited marked populations of dark blue-stained osteoblastic cells and bone matrix in and around the microbeads. Staining was less evident in microbeads cultured in growth medium (A_G, F_G, and C_G), and these samples also exhibited the light blue staining indicative of the original microbead matrix.

Tartrate-resistant acid phosphatase (TRAP, lower panels, Figure 5 M–R) is a marker for osteoclasts *in vivo*, and therefore indicates turnover and remodeling of bone. Similar to the staining results from Toluidine Blue O, the microbeads containing a combination of fresh BMMC and cultured MSC (F + C_O) exhibited the greatest amount of dark red TRAP-positive cell staining, compared to all other microbead implants. TRAP-positive staining was also evident in the microbeads containing fresh BMMC and cultured MSC that were maintained in osteogenic medium (F_O and C_O), however very little staining was observed in samples cultured in growth medium (A_G, F_G, and C_G).

Discussion

The major objective of this work was to compare the *in vivo* bone formation capacities of freshly isolated BMMC, culture-expanded MSC, and a combination of BMMC supplemented with MSC. We used a modular cell delivery system based on 3D collagen–chitosan microbeads in which cells were fully encapsulated, and which could be delivered to a subcutaneous site in the rat dorsum as an injectable implant. These microbeads have been shown to be supportive of MSC viability in previous studies (20,23), and in the present study both culture expanded MSC and those present in freshly isolated marrow were viable within microbeads over 17 days *in vitro* before being implanted. In addition, microbead types that were cultured in osteogenic medium (F_O, C_O, and F + C_O) became opaque over time in osteogenic culture, suggesting mineral deposition as observed in previous studies (20). Injection of microbead populations into the subcutaneous site using a fibrin hydrogel carrier was facile and allowed the examination of ectopic mineralized tissue formation. Overall, these results show that collagen–chitosan microbeads can support MSC viability and function, and can be used as a carrier system to deliver a variety of cell types in a minimally invasive manner.

A main finding in this study was that the combination of freshly isolated BMMC and culture-expanded MSC within osteogenically-differentiated microbeads had a strong positive and synergistic effect on ectopic bone formation *in vivo*, compared to either of the cell types, encapsulated alone. The combined cell treatment exhibited the highest average new bone volume, as confirmed by microCT and histological sectioning, as well as evidence of bone remodeling based on TRAP-positive staining. Freshly isolated bone marrow aspirate concentrates and bone marrow-derived mononuclear cells include a rich population of stem and progenitor cells, including hematopoietic, endothelial, and mesenchymal progenitor cells. These cell types can have potent paracrine actions and secrete a variety of factors that can stimulate or enhance bone formation and/or remodeling (29).

A small but crucial fraction of adult bone marrow consists of non-adherent hematopoietic-lineage stem and progenitor cells that are responsible for reconstituting the cellular components of blood. These cells also generate a complex network of soluble and paracrine signals which can regulate the survival, proliferation, and multidifferentiation ability of MSC (6–8). It is likely that these interactions were a source of the signals that caused the positive effects in relation to enhancing ectopic bone formation by microbeads containing both BMMC and MSC in this study. In particular, it has been reported that hematopoietic stem cells are able to guide mesenchymal differentiation toward the osteoblastic lineage *in vitro* (30) and potentiate bone formation *in vivo* (9) through the production of BMP-2 and BMP-6 (31). In addition, bone marrow-derived endothelial progenitor cells can migrate, proliferate, and secrete growth factors such as VEGF to enhance angiogenesis and subsequent bone formation (10,32).

Other bone marrow components of hematopoietic origin may also play an important role in enhancing osteogenesis. Platelets and megakaryocytes have been reported to stimulate differentiation of osteoprogenitors (33), and platelets are known to release growth factors, including PDGF, TGF-β, and VEGF, which have stimulatory effects on MSC, endothelial

cells, and osteoblasts (10). Additionally, macrophages and monocytes are osteoclast precursors, and are also modulators of the process of bone regeneration through secretion of osteotropic cytokines that induce blood-vessel formation or recruit marrow-derived progenitor cells to the ectopic bone site (34,35). In this study, the chitosan matrix may have played a role in activating the resident monocytes and macrophages to enhance bone tissue formation (36). While our data show that components of BMMC can potentiate ectopic bone formation, the identity of the stimulatory cell type was not specifically determined. However, therapies involving bone marrow fractions may therefore have a beneficial effect on bone regeneration.

It was clear in this study that the native MSC component of the BMMC implants alone was not a potent stimulator of ectopic bone formation. It has been estimated that only approximately 0.002% of the cells in BMMC are MSC (20,37-39), and therefore each subcutaneous implant of BMMC alone contained only about 60 MSC. While fresh bone marrow-derived MSC have been reported to have a higher *in vivo* osteogenic differentiation capacity than cultured MSC (6), the unpurified BMMC samples resulted in very modest formation of mineralized tissue. In the present study, supplementation of BMMC with 5×10^5 culture-expanded MSC encapsulated within microbeads caused a potent response. In a similar implant study using cell-seeded demineralized bone implants, it was suggested that fresh marrow cells contribute to intramembranous bone formation, while culture-expanded MSC resulted in endochondral ossification (29).

The observation of abundant TRAP-positive staining in implants containing both fresh BMMC and cultured MSC suggests that these implants were actively remodeling. The size and location of the TRAP-positive stained cells resembled the patterns expected from osteoclasts in contact with a biomaterial in a subcutaneous ectopic bone formation model (40). TRAP-positive staining is associated with osteoclasts, and it is well established that osteoclast-activated bone resorption is coupled with bone formation (41). Osteoclastic activity involves the release of matrix-associated growth factors that stimulate MSC and consequent bone formation. In turn, MSC and committed osteoblasts secrete both membrane-bound and soluble factors that contribute to the proliferation and the differentiation of multipotent osteoclast precursors. In our microbead implants containing both BMMC and MSC, the TRAP-positive stained osteoclasts derived from the BMMC component were active in remodeling the collagen-chitosan matrix, which in turn may have enhanced new bone formation by the culture-expanded MSC. Furthermore, microbead implants containing both BMMC and MSC (F + C_O) contained fewer fresh nucleated marrow cells compared to the microbead implants prepared with only fresh BMMC (F_C and F_O). Therefore, the greater amounts of TRAP-positive staining observed in the F + C_O implants clearly supports our conclusion of synergistic effects by the combination of fresh marrow cells and cultured MSC.

Interestingly, microbead implants containing culture-expanded but undifferentiated MSC resulted in no detected ectopic bone formation, despite being highly proliferative and viable prior to implant. It has been reported that undifferentiated MSC seeded on calcium phosphate bone grafts and implanted subcutaneously begin to disintegrate at day 3 and are completely absent by 14 days post-implantation (42). A similar study found that scaffolds

seeded with undifferentiated MSC were filled with only fibro-vascular tissue and produced no new bone formation over 4 weeks in a subcutaneous implant (19), and our recent work has also suggested that undifferentiated MSC can inhibit bone formation (43). In contrast, the osteogenically differentiated culture-expanded MSC in our study showed robust ectopic bone formation. Taken together, these data suggest that undifferentiated MSC may inhibit bone formation upon implantation, whereas pre-differentiated MSC are more likely to adapt to the implant environment and potentiate bone regeneration (44).

Acellular microbeads also demonstrated evident ectopic bone formation capacity, comparable to both the osteogenically differentiated BMMC and purified MSC implanted alone. This result demonstrates that the collagen–chitosan composite material is osteoconductive, and may in fact exhibit osteoinductive activity by recruiting host progenitor cells and stimulating bone formation at ectopic sites *in vivo* (45). Similar osteoconductive and osteoinductive effects of collagen–chitosan composites have been observed in previous studies (46). Bone formation by acellular microbeads in the present study also reinforces the concept that the presence of undifferentiated MSC is inhibitory to ectopic osteogenesis, since the material alone could clearly support bone formation but the presence of undifferentiated cells negated this effect.

In conclusion, this study shows that supplementation of a freshly isolated marrow preparation with cultured and predifferentiated MSC can potentiate ectopic bone formation when the combined cell preparation is delivered in collagen– chitosan microbeads. The combination of cell types showed a synergistic effect on the volume of bone formed and evidence of tissue remodeling. The collagen–chitosan material was mildly osteogenic in the absence of cells, and served as a practical and osteoconductive carrier for the encapsulated cells, while also allowing facile pre-culture and minimally invasive delivery. The microbead format allowed pre-culture and minimally invasive delivery of the cell-biomaterial therapy, and had also been used to create multiphase tissues designed to potentiate tissue vascularization (43,47,48). This cell delivery system may have utility as an alternative to current bone grafting materials in applications where potent and rapid bone regeneration is needed.

Acknowledgments

The Microscope and Image Analysis Laboratories (MIL) facility at the University of Michigan provided assistance with laser scanning confocal microscopy. In the Orthopaedic Research Laboratories at the University Michigan, Bonnie Nolan provided assistance with rat bone marrow harvesting, Kathy Sweet provided assistance with animal handling and *in vivo* implants, John Baker provided assistance with histology, and Basma Khoury, Dana Begun, and Ethan Daley provided assistance with microCT scanning and image/data analysis.

Research reported in this publication was supported in part by the “Large Bone Defect Healing (LBDH)” Consortium of the AO Foundation and by the National Institute of Arthritis and Musculoskeletal and Skin Diseases of the National Institutes of Health under award numbers R21AR062709 and R01AR062636. The content is solely the responsibility of the authors and does not necessarily represent the official views of the National Institutes of Health.

References

1. Stegemann JP, Verrier S, Gebhard F, Laschke MW, Martin I, Simpson H, Miclau T. Cell therapy for bone repair: narrowing the gap between vision and practice. Eur Cell Mater. 2014; 27:1–4.

2. Ciapetti G, Granchi D, Baldini N. The combined use of mesenchymal stromal cells and scaffolds for bone repair. Curr Pharm Des. 2012; 18:1796–1820. [PubMed: 22352754]

3. Lee K, Chan CK, Patil N, Goodman SB. Cell therapy for bone regeneration–bench to bedside. J Biomed Mater Res B Appl Biomater. 2009; 89:252–63. [PubMed: 18777578]

4. Caplan AI. Adult mesenchymal stem cells for tissue engineering versus regenerative medicine. J Cell Physiol. 2007; 21:341–47. [PubMed: 17620285]

5. Ikebe C, Suzuki K. Mesenchymal stem cells for regenerative therapy: optimization of cell preparation protocols. Biomed Res Int. 2014 951512 [about 11 p].

6. Banfi A, Muraglia A, Dozin B, Mastrogiacomo M, Cancedda R, Quarto R. Proliferation kinetics and differentiation potential of ex vivo expanded human bone marrow stromal cells: implications for their use in cell therapy. Exp Hematol. 2000; 28:707–15. [PubMed: 10880757]

7. Aubin JE. Osteoprogenitor cell frequency in rat bone marrow stromal populations: role for heterotypic cell–cell interactions in osteoblast differentiation. J Cell Biochem. 1999; 72:396–410. [PubMed: 10022521]

8. Baksh D, Davies JE, Zandstra PW. Soluble factor cross-talk between human bone marrow-derived hematopoietic and mesenchymal cells enhances *in vitro* CFU-F and CFU-O growth and reveals heterogeneity in the mesenchymal progenitor cell compartment. Blood. 2005; 106:3012–19. [PubMed: 16030193]

9. Jung Y, Song J, Shiozawa Y, Wang J, Wang Z, Williams B, Havens A, Schneider A, Ge C, Franceschi RT, McCauley LK, Krebsbach PH, Taichman RS. Hematopoietic stem cells regulate mesenchymal stromal cell induction into osteoblasts thereby participating in the formation of the stem cell niche. Stem Cells. 2008; 26:2042–51. [PubMed: 18499897]

10. Soltan M, Smiler D, Choi JH. Bone marrow: orchestrated cells, cytokines, and growth factors for bone regeneration. Implant Dent. 2009; 18:132–41. [PubMed: 19359864]

11. Bianco P. Minireview: the stem cell next door: skeletal and hematopoietic stem cell “niches” in bone. Endocrinology. 2011; 152:2957–62. [PubMed: 21610157]

12. Braccini A, Wendt D, Jaquiery C, Jakob M, Heberer M, Kenins L, Wodnar-Filipowicz A, Quarto R, Martin I. Three-dimensional perfusion culture of human bone marrow cells and generation of osteoinductive grafts. Stem Cells. 2005; 23:1066–72. [PubMed: 16002780]

13. Scaglione S, Braccini A, Wendt D, Jaquiery C, Beltrame F, Quarto R, Martin I. Engineering of osteoinductive grafts by isolation and expansion of ovine bone marrow stromal cells directly on 3D ceramic scaffolds. Biotechnol Bioeng. 2006; 93:181–87. [PubMed: 16245346]

14. Braccini A, Wendt D, Farhadi J, Schaeren S, Heberer M, Martin I. The osteogenicity of implanted engineered bone constructs is related to the density of clonogenic bone marrow stromal cells. J Tissue Eng Regen Med. 2007; 1:60–65. [PubMed: 18038393]

15. Boos AM, Loew JS, Deschler G, Arkudas A, Bleiziffer O, Gulle H, Dragu A, Kneser U, Horch RE, Beier JP. Directly auto-transplanted mesenchymal stem cells induce bone formation in a ceramic bone substitute in an ectopic sheep model. J Cell Mol Med. 2011; 15:1364–78. [PubMed: 20636333]

16. Kretlow JD, Spicer PP, Jansen JA, Vacanti CA, Kasper FK, Mikos AG. Uncultured marrow mononuclear cells delivered within fibrin glue hydrogels to porous scaffolds enhance bone regeneration within critical-sized rat cranial defects. Tissue Eng Part A. 2010; 16:3555–68. [PubMed: 20715884]

17. Chatterjea A, Renard AJ, Jolink C, van Blitterswijk CA, de Boer J. Streamlining the generation of an osteogenic graft by 3D culture of unprocessed bone marrow on ceramic scaffolds. J Tissue Eng Regen Med. 2012; 6:103–112. [PubMed: 21337706]

18. Kruyt MC, de Bruijn JD, Wilson CE, Oner FC, van Blitterswijk CA, Verbout AJ, Dhert WJ. Viable osteogenic cells are obligatory for tissue-engineered ectopic bone formation in goats. Tissue Eng. 2003; 9:327–36. [PubMed: 12740095]

19. Ye X, Yin X, Yang D, Tan J, Liu G. Ectopic bone regeneration by human bone marrow mononucleated cells, undifferentiated and osteogenically differentiated bone marrow mesenchymal stem cells in beta-tricalcium phosphate scaffolds. Tissue Eng Pt C. 2012; 18:545–56.

20. Wise JK, Alford AI, Goldstein SA, Stegemann JP. Comparison of uncultured marrow mononuclear cells and culture-expanded mesenchymal stem cells in 3D collagen–chitosan microbeads for orthopedic tissue engineering. Tissue Eng Part A. 2014; 20:210–24. [PubMed: 23879621]
21. Wang L, Stegemann JP. Thermogelling chitosan and collagen composite hydrogels initiated with beta-glycerophosphate for bone tissue engineering. Biomaterials. 2010; 31:3976–85. [PubMed: 20170955]
22. Wang L, Stegemann JP. Glyoxal crosslinking of cell-seeded chitosan/collagen hydrogels for bone regeneration. Acta Biomater. 2011; 7:2410–17. [PubMed: 21345389]
23. Wang L, Rao RR, Stegemann JP. Delivery of mesenchymal stem cells in chitosan/collagen microbeads for orthopedic tissue repair. Cells Tissues Organs. 2013; 197:333–43. [PubMed: 23571151]
24. Wise JK, Sumner DR, Virdi AS. Modulation of stromal cell-derived factor-1/CXC chemokine receptor 4 axis enhances rhBMP-2-induced ectopic bone formation. Tissue Eng Part A. 2012; 18:860–69. [PubMed: 22035136]
25. Owen ME, Cavé J, Joyner CJ. Clonal analysis *in vitro* of osteogenic differentiation of marrow CFU-F. J Cell Sci. 1987; 87:731–38. [PubMed: 3499442]
26. Ukai R, Honmou O, Harada K, Houkin K, Hamada H, Kocsis JD. Mesenchymal stem cells derived from peripheral blood protects against ischemia. J Neurotrauma. 2007; 24:508–20. [PubMed: 17402856]
27. Horn P, Bork S, Diehlmann A, Walenda T, Eckstein V, Ho AD, Wagner W. Isolation of human mesenchymal stromal cells is more efficient by red blood cell lysis. Cytotherapy. 2008; 10:676–85. [PubMed: 18985474]
28. Horn P, Bork S, Wagner W. Standardized isolation of human mesenchymal stromal cells with red blood cell lysis. Methods Mol Biol. 2011; 698:23–35. [PubMed: 21431508]
29. Claros S, Rodríguez-Losada N, Cruz E, Guerado E, Becerra J, Andrades JA. Characterization of adult stem/progenitor cell populations from bone marrow in a three dimensional collagen gel culture system. Cell Transplant. 2012; 21:2021–32. [PubMed: 22472743]
30. Liao J, Hammerick KE, Challen GA, Goodell MA, Kasper FK, Mikos AG. Investigating the role of hematopoietic stem and progenitor cells in regulating the osteogenic differentiation of mesenchymal stem cells *in vitro*. J Orthop Res. 2011; 29:1544–53. [PubMed: 21495066]
31. Shiozawa Y, Jung Y, Ziegler AM, Pedersen EA, Wang J, Wang Z, Song J, Wang J, Lee CH, Sud S, Pienta KJ, Krebsbach PH, Taichman RS. Erythropoietin couples hematopoiesis with bone formation. PLoS One. 2010; 5:e10853. [PubMed: 20523730]
32. Amini AR, Laurencin CT, Nukavarapu SP. Bone tissue engineering: recent advances and challenges. Crit Rev Biomed Eng. 2012; 40:363–408. [PubMed: 23339648]
33. Friedenstein AJ, Latzinik NV, Gorskaya YuF, Luria EA, Moskvina IL. Bone marrow stromal colony formation requires stimulation by haemopoietic cells. Bone Miner. 1992; 18:199–213. [PubMed: 1392694]
34. Soltan M, Rohrer MD, Prasad HS. Monocytes: super cells for bone regeneration. Implant Dent. 2012; 21:13–20. [PubMed: 22214990]
35. Dong L, Wang C. Harnessing the power of macrophages/monocytes for enhanced bone tissue engineering. Trends Biotechnol. 2013; 31:342–46. [PubMed: 23623371]
36. Lee CG, Da Silva CA, Lee JY, Hartl D, Elias JA. Chitin regulation of immune responses: an old molecule with new roles. Curr Opin Immunol. 2008; 20:684–89. [PubMed: 18938241]
37. Friedenstein AJ, Chailakhyan RK, Gerasimov UV. Bone marrow osteogenic stem cells: in vitro cultivation and transplantation in diffusion chambers. Cell Tissue Kinet. 1987; 20:263–72. [PubMed: 3690622]
38. Pittenger MF, Mackay AM, Beck SC, Jaiswal RK, Douglas R, Mosca JD, Moorman MA, Simonetti DW, Craig S, Marshak DR. Multilineage potential of adult human mesenchymal stem cells. Science. 1999; 284:143–47. [PubMed: 10102814]
39. Alvarez-Viejo M, Menendez-Menendez Y, Blanco-Gelaz MA, Ferrero-Gutierrez A, Fernandez-Rodriguez MA, Gala J, Otero-Hernandez J. Quantifying mesenchymal stem cells in the mononuclear cell fraction of bone marrow samples obtained for cell therapy. J Transplant Proc. 2013; 45:434–39.

40. Trojani C, Boukhechba F, Scimeca JC, Vandenbos F, Michiels JF, Daculsi G, Boileau P, Weiss P, Carle GF, Rochet N. Ectopic bone formation using an injectable biphasic calcium phosphate/Si-HPMC hydrogel composite loaded with undifferentiated bone marrow stromal cells. Biomaterials. 2006; 27:3256–64. [PubMed: 16510180]

41. Martin T, Gooi JH, Sims NA. Molecular mechanisms in coupling of bone formation to resorption. Crit Rev Eukaryot Gene Expr. 2009; 19:73–88. [PubMed: 19191758]

42. Zimmermann CE, Gierloff M, Hedderich J, Açil Y, Wiltfang J, Terheyden H. Survival of transplanted rat bone marrow-derived osteogenic stem cells *in vivo*. Tissue Eng Part A. 2011; 17:1147–56. [PubMed: 21142699]

43. Rao RR, Vigen ML, Peterson AW, Caldwell DJ, Putnam AJ, Stegemann JP. Dual-phase osteogenic and vasculogenic engineered tissue for bone formation. Tissue Eng Part A. 2015; 21:530–40. [PubMed: 25228401]

44. Peters A, Toben D, Lienau J, Schell H, Bail HJ, Matziolis G, Duda GN, Kaspar K. Locally applied osteogenic predifferentiated progenitor cells are more effective than undifferentiated mesenchymal stem cells in the treatment of delayed bone healing. Tissue Eng Pt A. 2009; 15:2947–54.

45. Miron RJ, Zhang YF. Osteoinduction: a review of old concepts with new standards. J Dent Res. 2012; 91:736–44. [PubMed: 22318372]

46. Kung S, Devlin H, Fu E, Ho KY, Liang SY, Hsieh YD. The osteoinductive effect of chitosan–collagen composites around pure titanium implant surfaces in rats. J Periodontal Res. 2011; 46:126–33. [PubMed: 21108645]

47. Caldwell DJ, Rao RR, Stegemann JP. Assembly of discrete collagen–chitosan microenvironments into multiphase tissue constructs. Adv Healthc Mater. 2013; 2:673–77. [PubMed: 23184758]

48. Peterson AW, Caldwell DJ, Rioja AY, Rao RR, Putnam AJ, Stegemann JP. Vasculogenesis and angiogenesis in modular collagen-fibrin microtissues. Biomater Sci. 2014; 2:1497–1508. [PubMed: 25177487]

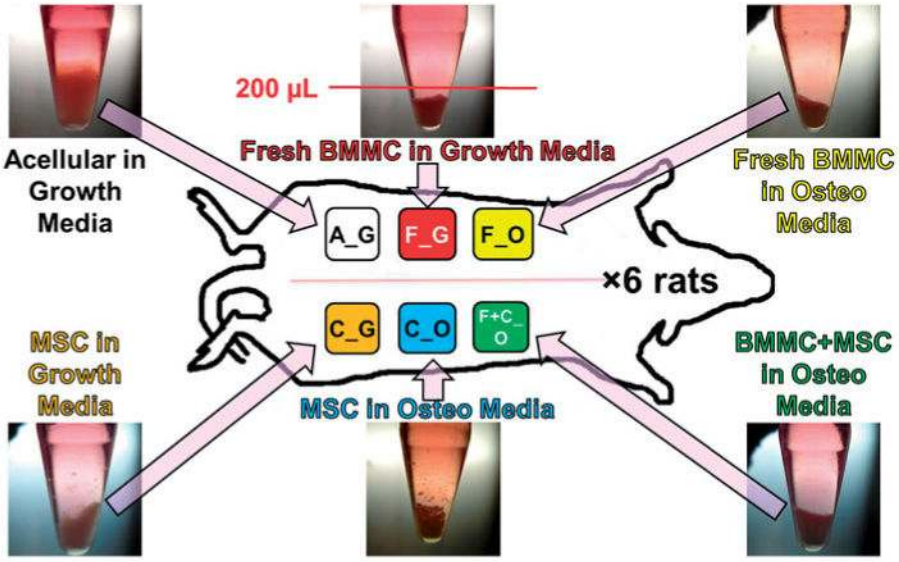

Figure 1.

Schematic of microbead implants in rat subcutaneous dorsum. Microbeads cultured for a total of 20 days ($n = 6$, shown in photos of centrifuge tube cultures) were subsequently mixed with 500 µl of fibrin gel carrier and injected subcutaneously in rat dorsum. Microbead implant types, according to type of encapsulated cells and culture media, were A_G, F_G, F_O, C_G, C_O, and F+C_O, where A = acellular; F = freshly isolated BMMC; C = culture-expanded MSC; G = growth medium, O = osteogenic medium. Ectopic implants were harvested at 5-weeks, and analyzed by microCT and histology.

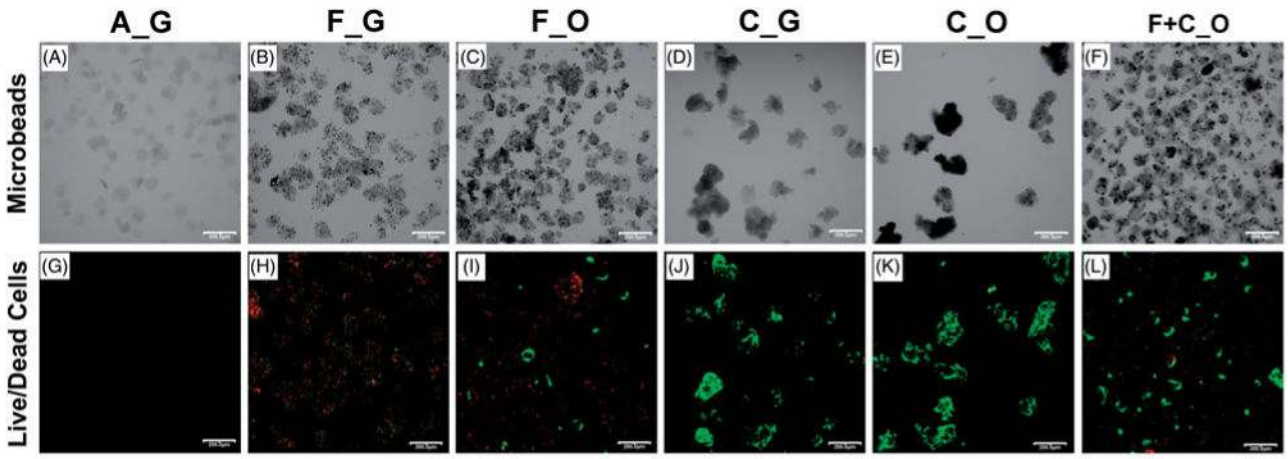

Figure 2.

Morphology and viability of cell-encapsulating microbeads. Cell-encapsulating microbeads, to be used as implants *in vivo*, were cultured *in vitro* in control MSC growth media for an initial 3 days, and then in either growth or osteogenic media for an additional 17 days. At day 17 of *in vitro* culture, microbeads were imaged by transmitted light (A–F), and green fluorescently labeled live cells and red fluorescently labeled dead cells were imaged to assess cell viability (G–L). Microbead types, according to type of encapsulated cells and culture media, were A_G, F_G, F_O, C_G, C_O, and F+C_O, where A = acellular; F = freshly isolated BMMC; C = culture-expanded MSC; G = growth medium, O = osteogenic medium. Scale bar = 200 μm. Images best viewed in color.

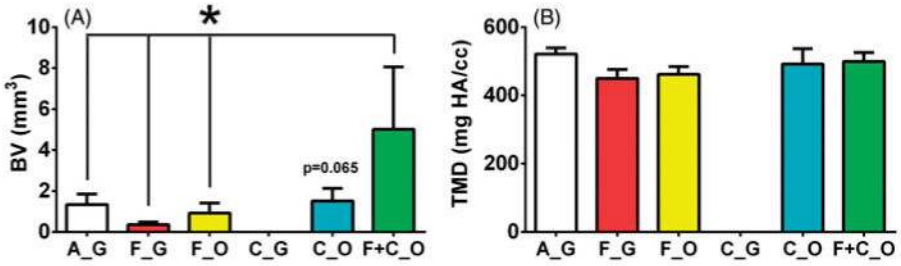

Figure 3.

Bone volume and tissue mineral density of 5-week ectopic microbead implants. (A) Bone volume (BV) and (B) tissue mineral density (TMD) of cell-microbead containing ectopic implants at 5-weeks. Microbead implant types, according to type of encapsulated cells and culture media, were A_G, F_G, F_O, C_G, C_O, and F + C_O, where A = acellular; F = freshly isolated BMMC; C = culture-expanded MSC; G = growth medium, O = osteogenic medium. $n \geq 5$. $^{*}p \leq 0.05$. There was a lack of bone formation detected in C_G microbead implants.

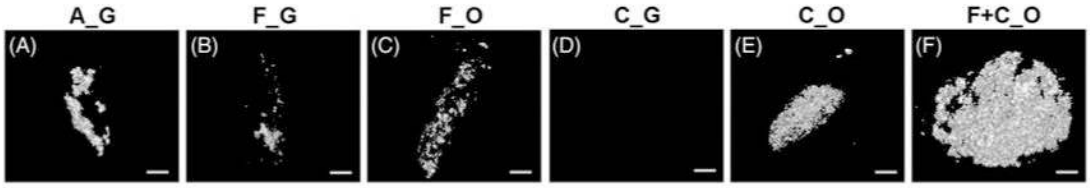

Figure 4.

Reconstructed 3D microCT images of representative 5-week ectopic microbead implants. Microbead implant types, according to type of encapsulated cells and culture media, were A_G (A), F_G (B), F_O (C), C_G (D), C_O (E), and F +C_O (F), where A = acellular; F = freshly isolated BMMC; C = culture-expanded MSC; G = growth medium, O = osteogenic medium. Scale bar = 1 mm for all images. There was a lack of bone formation detected in C_G microbead implants.

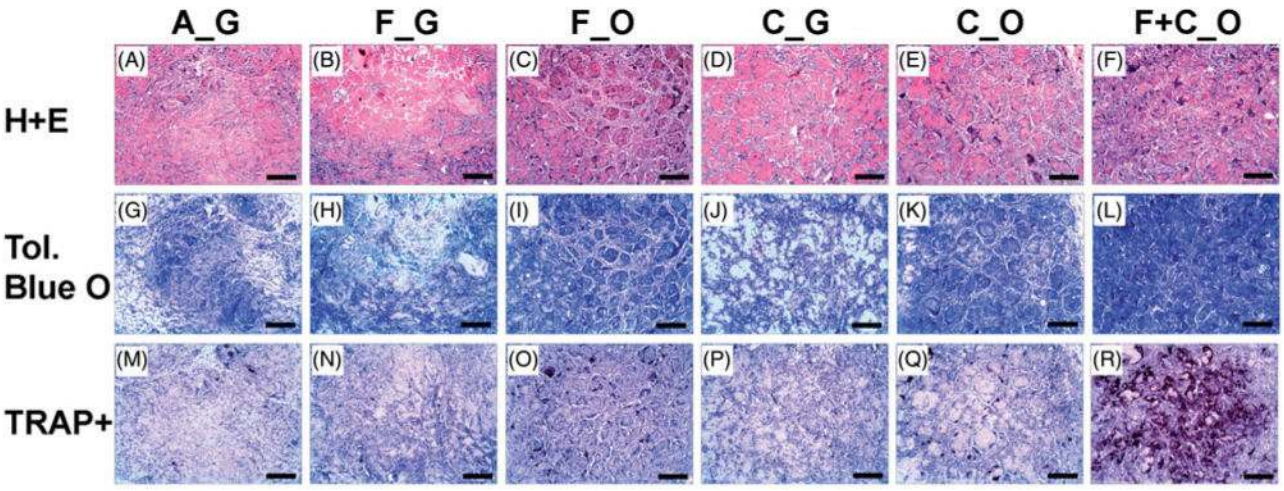

Figure 5.

Histology of 5-week ectopic microbead implants. Representative views of sections (7 μm) of microbead implants stained with Hematoxylin and Eosin (H + E), Toluidine Blue O (Tol. Blue O), or for tartrate-resistant acid phosphatase positive cells (TRAP+). Microbead types of each implant, according to type of encapsulated cells and culture media, were A_G, F_G, F_O, C_G, C_O, and F + C_O, where A = acellular; F = freshly isolated BMMC; C = culture-expanded MSC; G = growth medium, O = osteogenic medium. Scale bar = 200 μm. Images best viewed in color.